photonics

MDPI

Article

Fabrication of 2 kW-Level Chirped and Tilted Fiber Bragg Gratings and Mitigating Stimulated Raman Scattering in Long-Distance Delivery of High-Power Fiber Laser

Xiaofan Zhao [1,2,†], Xin Tian [1,3,†], Meng Wang [1,2,3], Binyu Rao [1,2], Hongye Li [1,3], Xiaoming Xi [1,2,3] and Zefeng Wang [1,2,3,*]

[1] College of Advanced Interdisciplinary Studies, National University of Defense Technology, Changsha 410073, China; zhaoxiaofan_zxf@nudt.edu.cn (X.Z.); tianxin@nudt.edu.cn (X.T.); wangmeng@nudt.edu.cn (M.W.); raobinyu@nudt.edu.cn (B.R.); lihongye@nudt.edu.cn (H.L.); xixiaoming@nudt.edu.cn (X.X.)
[2] Hunan Provincial Key Laboratory of High Energy Laser Technology, Changsha 410073, China
[3] State Key Laboratory of Pulsed Power Laser Technology, Changsha 410073, China
* Correspondence: zefengwang@nudt.edu.cn
† These authors contributed equally to this work.

Abstract: Chirped and tilted fiber Bragg gratings (CTFBGs) have attracted a lot of attention in stimulated Raman scattering (SRS) suppression of high-power fiber lasers. However, the laser power handling capacity seriously limits their applications. In this paper, by optimizing the inscription parameters and post-processing strategy, we fabricate a large-mode-area double-cladding CTFBG with a thermal slope of ~0.015 °C/W due to the low insertion loss of about 0.15 dB, which make it possible for direct kilowatt-level application. A 2 kW-level fiber laser oscillator is employed to test the CTFBG, and a series of experiments have been carried out to compare the effect of SRS mitigation in high-power fiber laser long-distance delivery. In addition, the influence of CTFBGs on laser beam quality is studied for the first time. Experimental results indicated that the CTFBG could effectively mitigate SRS and has no obvious influence on laser beam quality. This work opens a new opportunity for further power scaling and the delivery of high-power fiber lasers over longer distances.

Keywords: high-power fiber lasers; chirped and tilted fiber Bragg gratings; stimulated Raman scattering; laser beam quality

Citation: Zhao, X.; Tian, X.; Wang, M.; Rao, B.; Li, H.; Xi, X.; Wang, Z. Fabrication of 2 kW-Level Chirped and Tilted Fiber Bragg Gratings and Mitigating Stimulated Raman Scattering in Long-Distance Delivery of High-Power Fiber Laser. *Photonics* **2021**, *8*, 369. https://doi.org/10.3390/photonics8090369

Received: 4 August 2021
Accepted: 30 August 2021
Published: 2 September 2021

1. Introduction

High-power fiber lasers have been widely used in lots of areas, such as industrial processing, medical treatment, material research, defense technology, and so on, due to their diffraction-limited beam quality, compactness, high efficiency, stability, and robustness [1–3]. In the past decade, thanks to the fast development of high-brightness laser diodes (LDs) and large-mode-area (LMA) fibers, the output power of fiber lasers has experienced an outstanding increase and promoted the rapid development of advanced manufacturing [4–6] of material processing and defense technology. However, SRS is still one of the primary limitations on further power scaling and the long-distance delivery of high-power fiber laser [7,8]. Once SRS effect occurs, the laser power would convert to Raman Stokes light, which obstructs the increase of the signal power. Meanwhile, the backward Stokes lights are a serious threat to the system. Thus, suppressing SRS has become an essential task in high-power fiber laser systems.

So far, several methods for SRS suppression have been proposed, such as enlarging the fiber mode area using LMA fibers [9], spectrally selective fibers [10], and fiber spectral filters like long-period fiber gratings (LPFGs) and CTFBGs [11–13]. However, LMA fibers must be combined with hard controlling numerical aperture for the operation of fundamental mode. Too large of a core diameter will decrease the transverse mode instability (TMI) threshold

in gain fibers, which is another important power scaling limitation [14]. Spectrally selective fibers usually possess complex design, high cost, and are limited by the maximum fiber core size that can be employed. CTFBGs and LPFGs as fiber spectral filters can couple core modes into cladding modes, realizing the filtering of Stokes light, and are quite easy to design and fabricate. However, for LPFGs, the instability resulting from cross-sensitivity is the most important fact limiting their applications [15]. In comparison, CTFBGs possess better stability and have been intensively studied in the past few years [16–20]. Although good SRS suppression have been obtained in many high-power fiber laser systems, in most cases CTFBGs were inserted between the seed and the amplification-stage in master oscillator power-amplifier (MOPA) systems [21,22], which is mainly limited by the power handling capacity. For the commonly used ultraviolet (UV) inscription technology, the residual hydrogen, thermal stress, and other defects will cause a large amount of heat in CTFBGs when working at a high-power level [22].

In this paper, to relieve the heat of CTFBGs, the UV inscription parameters are optimized and some post-process strategies are used in fabrication. By this way, a 2 kW-level CTFBG has been designed and inscribed on GDF-20/400 LMA fiber through the phase-mask method. As several annealing processes are carried out to enhance the power handling capacity, the CTFBG has a low measured signal insertion loss of about 0.15 dB, resulting in a small thermal slope of ~0.015 °C/W. To test the CTFBG, a series of comparative experiments have been carried out to mitigate the SRS in high-power fiber laser long-distance delivery. By changing the position of the CTFBG in the 20 m delivering fibers, a maximum SRS suppression ratio bigger than 20 dB is obtained. In addition, the influence of the CTFBG on the laser beam quality (LBQ) is also studied. Results show that the CTFBG have few influences on LBQ, which is useful for the longer delivery distance of high-power fiber lasers.

2. Fabrication of High-Power CTFBGs

CTFBGs are a kind of band-stop filters, which combines the characteristics of chirped fiber Bragg grating (CFBG) and tilted fiber Bragg grating (TFBG). As the structure shown in Figure 1, CTFBGs can couple the core modes with the backward cladding modes, which can filter the Stokes light within the stop-band into the cladding, and then be leaked into the air. By choosing the proper tilt angle, chirp rate, grating length, and modulation depth, suitable CTFBGs can be acquired.

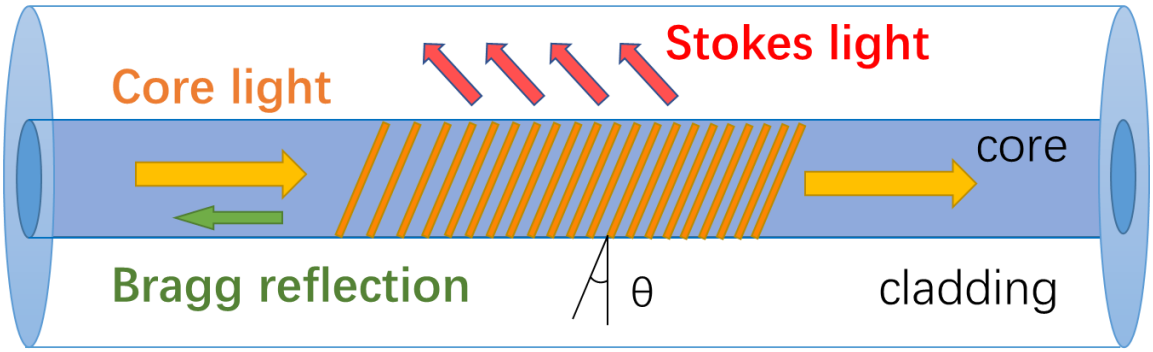

Figure 1. The structure and operating mechanism of CTFBGs for Raman signal filtering.

The CTFBG was inscribed by a 248 nm excimer UV laser source with pulse energy of 6 mJ based on phase mask inscription technique. The beam was focused by a cylindrical lens with a focal length of 150 mm on the LMA-GDF-20/400 GDF fiber through a 4.7°-tilted phase mask as shown in Figure 2a,b. The phase mask had the central period of 791 nm and a chirp rate of 0.4 nm/cm and the inscribed CTFBGs would have a tilted angle of 6.8° with central wavelength of around 1135 nm on the transmission spectra. Before the inscription, the fiber should be hydrogen-loaded for 8 weeks under pressure of 16 MPa to enhance

photon-sensitivity [23]. During the inscribing process, an optical spectrum analyzer (OSA) with wide band light source was applied to monitor the resonance wavelength and depth. The recording lasted for 20 min with a repetition rate of 100 Hz. The typical index modulation depth was 10^{-3}, and the spectral shape indicated that its uniformity over the grating length of 35 mm was fine. After inscription, the grating needs further post-processing to release the thermal stress and remove the residual hydrogen, which will cause a large amount of heat while operating [22]. After step annealing and packaging, this CTFBG can operate at 2 kW power level. Additionally, through a series annealing process, which could be seen as an accelerated aging test, the characteristics of the CTFBG tended to be stable. The following burn-in test and high-power experiments also indicated a long-term stability of the CTFBG.

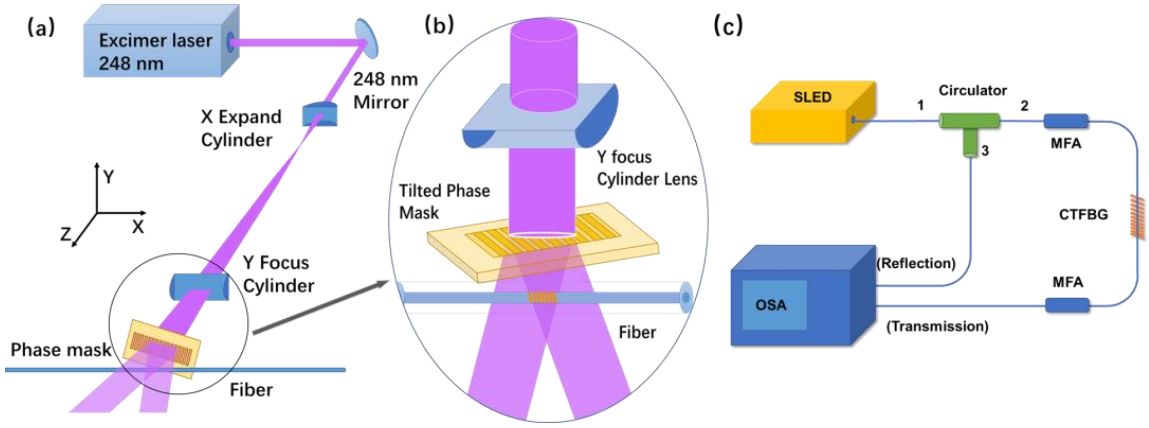

Figure 2. (**a**) The schematic diagram of the inscription system; (**b**) the partial enlarged view; (**c**) the schematic diagram of the spectra test system.

The transmission and reflection spectra were measured through the setup shown in Figure 2c. A super light-emitting diode (SLED) source was used in the setup, and the CTFBG was connected with port 2 of the optic circulator. Two mode field adaptors (MFAs) were applied to connect different fibers. The transmission and reflection spectra could be measured in port 2 and port 3, respectively. The transmission spectra were measured online during inscription. As shown in Figure 3, the center wavelength of the coupled cladding modes is 1134.67 nm, and the 3 dB bandwidth is about 8.58 nm, which is mainly limited by the grating length and can be greatly widened by increasing the grating length using a longer phase mask in the future. The maximum rejection ratio at 1134.67 nm is about 15 dB, and the residual Bragg reflection near 1151.5 nm (theoretically design value) was too weak to be observed. On account of the small tilted angle of the grating plane, the CTFBG had low response to polarization [24,25] because the orders of mainly coupled cladding modes were not high enough.

To test the power handling capacity of the CTFBG, a 2 kW-level fiber laser oscillator operating at 1080 nm was employed. As shown in Figure 4a, a gain fiber with core/cladding diameters of 20/400 μm was pumped by LDs working at 976 nm in a forward pumping structure. The measured insertion loss of the CTFBG for the signal laser is shown in Figure 4b, and the average value is 3.07%, corresponding to about 0.15 dB. Figure 4c shows the temperature image recorded by a thermal camera when laser power was 1935 W. It can be seen that the temperature distribution along the CTFBG is relatively uniform, and the maximum value is about 52 °C with a thermal slope of ~0.015 °C/W. The thermal image indicated there are no defects along the CTFBG, and the heat should be mainly caused by the inscription technology, as well as residual hydrogen and -OH-related chemical bonds [22].

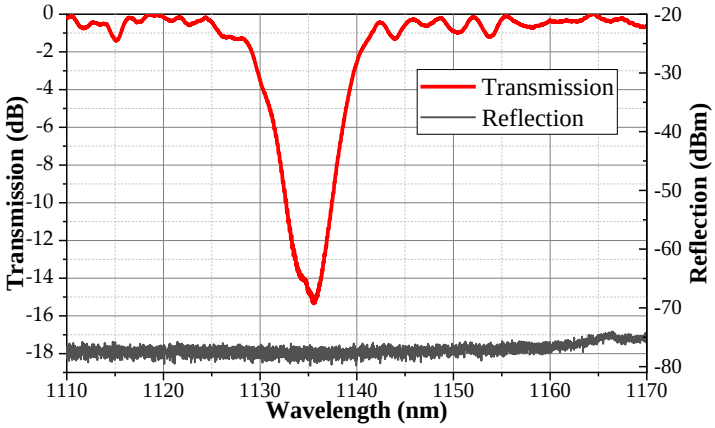

Figure 3. The tested spectra of the CTFBG.

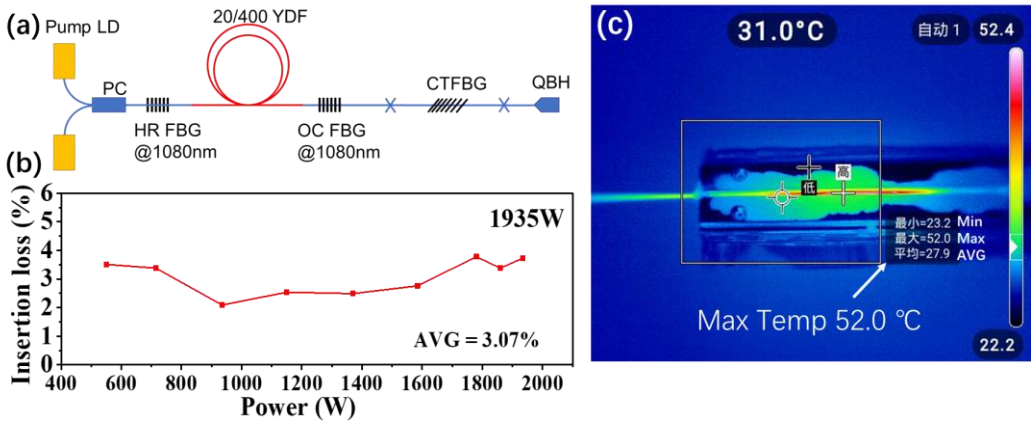

Figure 4. (**a**) Test system for the power handling capacity of the CTFBG; (**b**) the measured insertion loss for signal laser; (**c**) thermal image of the CTFBG at 1935 W.

3. SRS Mitigation for High-Power Fiber Laser Delivery

To research the SRS mitigation effect of the CTFBG in high-power fiber laser long-distance delivery, a 20 m passive fiber (LMA-GDF-20/400) was added following the OC FBG as the Raman gain media. The passive fiber was sliced into 5 m and 15 m for four comparative experiments with the CTFBG inserted into four different positions as shown in Figure 5a–d. The output spectrum of the oscillator with the 20 m delivery fiber but without the CTFBG is shown in Figure 6 as a criterion for the following comparison. It can be seen that the Raman isolation had reached −21.8 dB at output power of 1537 W. For safety reasons, the oscillator output laser power was not increased beyond this value (1537 W) in the experiments.

The measured output spectrum and beam qualities under the four setups are shown in Figure 7a–d, corresponding to Setup I to IV, respectively. For better comparison, in experiments all of the four setups worked at the same current of pump LDs as the 2-kW oscillator with 20 m delivery fibers. The results showed that the final output powers and the maximum Raman suppression ratios changed with the insertion position of the CTFBG. The output powers reached 1438 W, 1529 W, 1408 W, and 1438 W, while the maximum Raman isolation ratio of −31.8 dB, −33.9 dB, −34.6 dB, and −36.7 dB were acquired in Setup I to Setup IV, respectively. Because the function of the CTFBG is filtering, the Raman suppress effects and the output power would change in different insertion positions of the CTFBG by retarding the accumulation of the SRS along the fiber to different degrees [18]. Therefore, a

better insertion position could be obtained through the comparison experiments, as well as the chance of longer laser delivery distance.

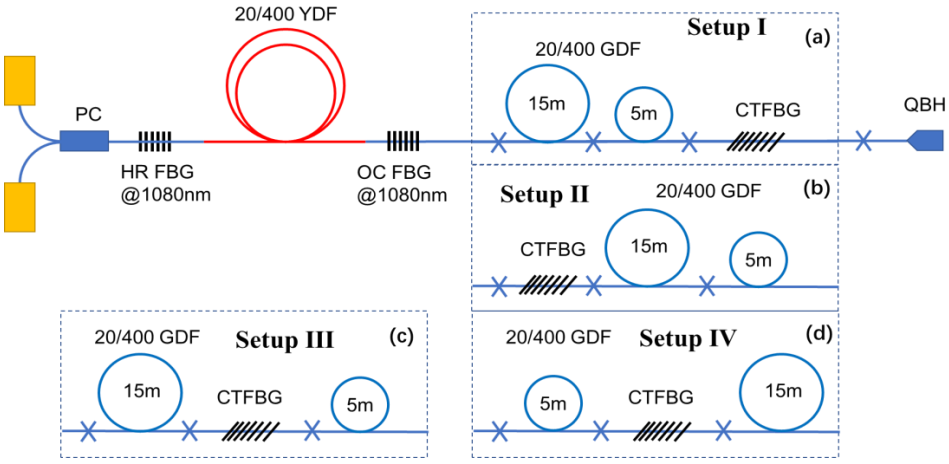

Figure 5. Four comparative experimental setups with different positions of the CTFBG and the output spectra of the oscillator. (**a**) Setup I: after 20 m delivery fiber; (**b**) Setup II: before 20 m delivery fiber; (**c**) Setup III: between 15 m and 5 m delivery fiber; (**d**) Setup IV: between 5 m and 15 m delivery fiber.

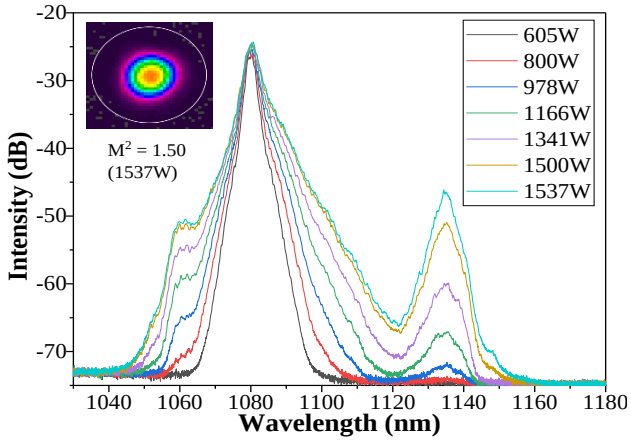

Figure 6. Output spectrum of the fiber oscillator with 20 m delivery fiber but without the CTFBG.

The SRS isolation rates and final output powers of different setups are compared in Figure 8a,b. The subtracted spectra between the setups without and with CTFBG also showed similarity with the transmission spectrum of the CTFBG. All the setups showed that the CTFBG had an effective mitigation on the Stokes light of SRS. Among the four setups, the CTFBG had the highest maximum Raman isolation ratio and a relatively small decrease in output power when the CTFBG was inserted between 5 m and 15 m delivery fibers as Setup IV. When the CTFBG was inserted before the 20 m delivery fiber in Setup II, it had the lowest decrease in output power. Considering the insertion loss of the CTFBG and the additional fuse point, the CTFBG was capable of mitigating the power consumption of the SRS. Additionally, the fiber laser itself could also output more power safely with the backward Stokes light suppressed. Thus, the delivery distance of the fiber laser would be longer at the same SRS signal intensity level while maintaining output power. Besides, due to the delivery fiber being Raman gain material hat would consume the signal power after the oscillator and convert it to Raman signal, it was inevitable to get lower output signal power with longer delivery distance. Still, there would be a proper position of applying the CTFBG to balance the SRS mitigation and output power. Meanwhile, the beam qualities of different setups were also compared in Figure 8c to test the influence of CTFBGs on beam quality. The figure shows the beam qualities M2 fluctuated around 1.6. In consideration of

the influence induced by fuse points, a contrast experiment was carried out under the same fusing conditions to test the influence of the fuse points with different fusing states on beam qualities and insertion loss as a reference in Figure 8d. Point 1 and 2 were normally fused, and Point 3 was badly fused with a little mismatch added manually during the fusing process to give different fusing state. The consequence showed the influence of fuse points was enormous, and a normal fuse point might cause beam quality deterioration of around a 0.1 increase in M2. Besides, the fuse points would also induce considerable additional insertion loss to the fiber laser systems. According to the contrast experiment, it is inferred that the CTFBGs exert little influence on beam quality.

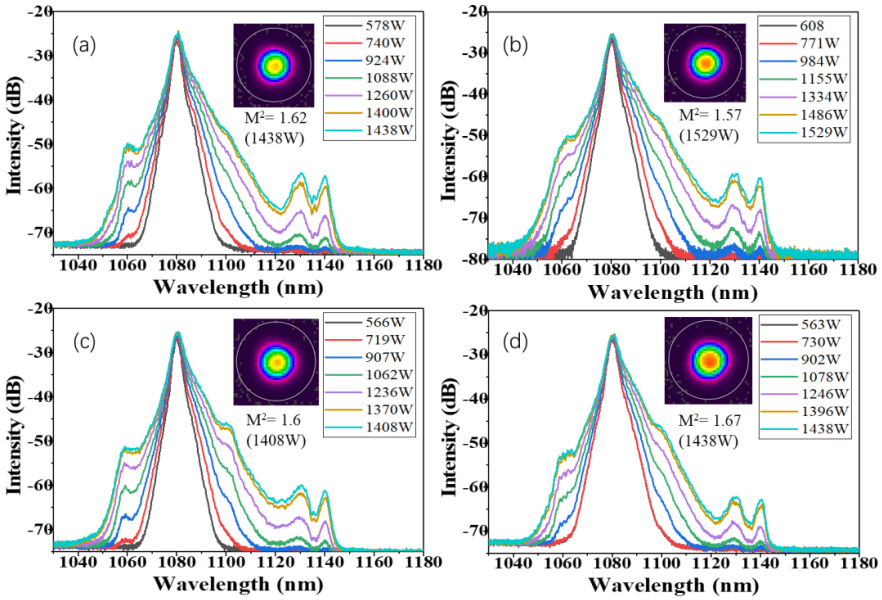

Figure 7. Output spectra of the oscillator corresponding to the four setups in Figure 6: (**a**) Setup I; (**b**) Setup II; (**c**) Setup III; (**d**) Setup IV.

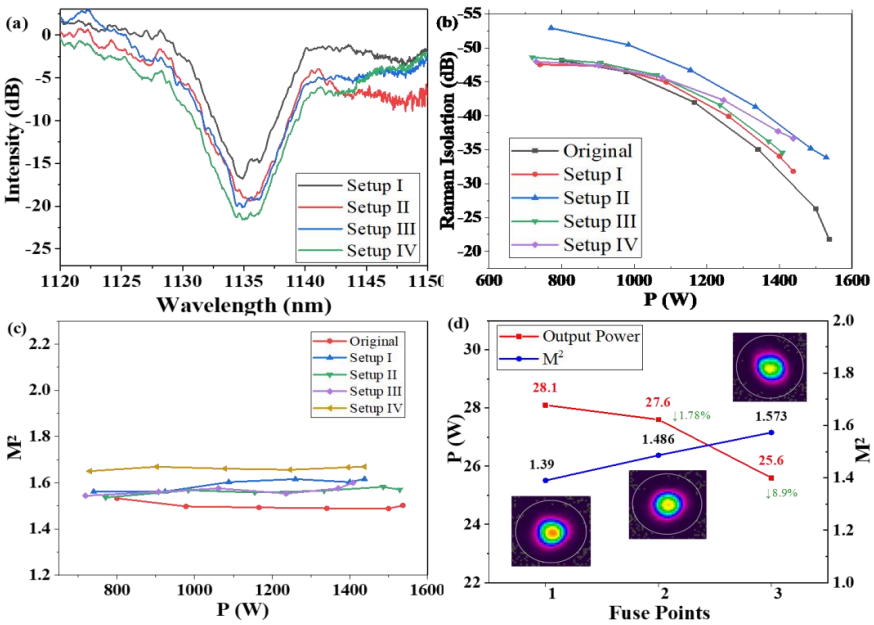

Figure 8. (**a**) The measured rejection spectra of the CTFBG with different positions; (**b**) maximum SRS isolation ratio with output power in different setups; (**c**) beam quality M2 in different setups; (**d**) influence of the fuse points on M2 and insertion loss.

4. Conclusions

In conclusion, we have designed and fabricated a 2-kW level CTFBG by optimizing the inscription parameters and adopting several post-processing strategies. The CTFBG has a low insertion loss of ~0.15 dB, resulting in a small thermal slope of ~0.015 °C/W. The maximum rejection depth at ~1135 nm is bigger than 15 dB, while the 3 dB bandwidth is only 8.58 nm, which is mainly limited by the grating length. In addition, the residual Bragg reflection near 1151.5 nm is too weak to be observed, which is very beneficial for SRS suppression. To test the CTFBG, a 2-kW level fiber oscillator system was employed and a series of comparative experiments were carried out. The results not only indicate that the CTFBG has effectively suppressed SRS but also has no obvious influence on LBQ, which is very useful for longer delivery distance of high-power fiber lasers. In the future, CTFBGs with wider rejection band, bigger filtering depth, and higher power handling capacity can be achieved by further optimizing the inscription parameters, with a suitable phase mask of longer grating length and proper chirp ratio.

Author Contributions: Writing original draft, X.Z.; Investigation, X.Z. and X.T.; Methodology, X.Z. and Z.W.; Data curation, X.T., M.W., B.R., H.L. and X.X.; Formal analysis, X.T., B.R., H.L. and X.X.; Funding acquisition, M.W. and Z.W.; Project administration, X.X. and Z.W.; Resources, M.W. and Z.W.; Supervision, Z.W.; Writing review & editing, X.T. and M.W. All authors have read and agreed to the published version of the manuscript.

Funding: This work was supported by the Outstanding Youth Science Fund Project of Hunan Province Natural Science Foundation (2019JJ20023) and the National Natural Science Foundation of China (NSFC) (11974427, 12004431), and State Key Laboratory of Pulsed Power Laser (SKL2020ZR05, SKL2021ZR01).

Conflicts of Interest: The authors declare no conflict of interest.

References

1. Richardson, D.J.; Nilsson, J.; Clarkson, W.A. High power fiber lasers: Current status and future perspectives. *J. Opt. Soc. Am. B* **2010**, *27*, B63–B92. [CrossRef]
2. Nilsson, J.; Ramachandran, S.; Shay, T.; Shirakawa, A. High-power fiber lasers. *IEEE J. Sel. Top. Quantum Electron.* **2009**, *15*, 1–2. [CrossRef]
3. Jauregui, C.; Limpert, J.; Tünnermann, A. High-power fibre lasers. *Nat. Photon.* **2013**, *7*, 861–867. [CrossRef]
4. Ikoma, S.; Uchiyama, K.; Takubo, Y.; Kashiwagi, M.; Shima, K.; Tanaka, D. 5-kW single stage all-fiber Yb-doped single-mode fiber laser for materials processing. In Proceedings of the Conference on Fiber Lasers XV: Technology and Systems SPIE, San Francisco, CA, USA, 26 February 2018; Volume 10512, p. 11.
5. Wang, Y.; Kitahara, R.; Kiyoyama, W.; Shirakura, Y.; Kurihara, T.; Nakanishi, Y.; Yamamoto, T.; Nakayama, M.; Ikoma, S.; Shima, K. 8-kW single-stage all-fiber Yb-doped fiber laser with a BPP of 0.50 mm-mrad. In Proceedings of the Conference on Fiber Lasers XVII: Technology and Systems SPIE, San Francisco, CA, USA, 21 February 2020; Volume 11260, p. 74.
6. Krämer, R.G.; Möller, F.; Matzdorf, C.; Goebel, T.A.; Strecker, M.; Heck, M.; Richter, D.; Plötner, M.; Schreiber, T.; Tünnermann, A.; et al. Extremely robust femtosecond written fiber Bragg gratings for an ytterbium-doped fiber oscillator with 5 kW output power. *Opt. Lett.* **2020**, *45*, 1447–1450. [CrossRef] [PubMed]
7. Otto, H.-J.; Jauregui, C.; Limpert, J.; Tünnermann, A. Average power limit of fiber-laser systems with nearly diffrac-tion-limited beam quality. In Proceedings of the Conference on Fiber Lasers XIII: Technology, Systems, and Applications, San Francisco, CA, USA, 9 March 2016; Volume 9728, p. 97280E.
8. Wang, Y.; Xu, C.-Q.; Po, H. Analysis of Raman and thermal effects in kilowatt fiber lasers. *Opt. Commun.* **2004**, *242*, 487–502. [CrossRef]
9. Stutzki, F.; Jansen, F.; Otto, H.-J.; Jauregui, C.; Limpert, J.; Tünnermann, A. Designing advanced very-large-mode-area fibers for power scaling of fiber-laser systems. *Optica* **2014**, *1*, 233–242. [CrossRef]
10. Kim, J.; Dupriez, P.; Codemard, C.; Nilsson, J.; Sahu, J.K. Suppression of stimulated Raman scattering in a high power Yb-doped fiber amplifier using a W-type core with fundamental mode cut-off. *Opt. Express* **2006**, *14*, 5103–5113. [CrossRef]
11. Nodop, D.; Jauregui, C.; Jansen, F.; Limpert, J.; Tünnermann, A. Suppression of stimulated Raman scattering employing long period gratings in double-clad fiber amplifiers. *Opt. Lett.* **2010**, *35*, 2982–2984. [CrossRef]
12. Wang, M.; Zhang, Y.; Wang, Z.; Sun, J.; Cao, J.; Leng, J.; Gu, X.; Xu, X. Fabrication of chirped and tilted fiber Bragg gratings and suppression of stimulated Raman scattering in fiber amplifiers. *Opt. Express* **2017**, *25*, 1529–1534. [CrossRef]
13. Wang, M.; Li, Z.; Liu, L.; Wang, Z.; Gu, X.; Xu, X. Fabrication of chirped and tilted fiber Bragg gratings on large-mode-area doubled-cladding fibers by phase-mask technique. *Appl. Opt.* **2018**, *57*, 4376–4380. [CrossRef] [PubMed]

14. Jauregui, C.; Eidam, T.; Otto, H.-J.; Stutzki, F.; Jansen, F.; Limpert, J.; Tünnermann, A. Temperature-induced index gratings and their impact on mode instabilities in high-power fiber laser systems. *Opt. Express* **2012**, *20*, 440–451. [CrossRef]
15. Shen, H.; Jiao, K.; Guan, Z.; Yang, F.; Zhu, R. Suppressing stimulated Raman scattering in high-power continuous-wave fiber lasers based on long-period fiber grating. *Optics Express* **2020**, *28*, 6048–6063.
16. Wang, M.; Wang, Z.; Liu, L.; Hu, Q.; Xiao, H.; Xu, X. Effective suppression of stimulated Raman scattering in half 10 kW tandem pumping fiber lasers using chirped and tilted fiber Bragg gratings. *Photonics Res.* **2019**, *7*, 167–171. [CrossRef]
17. Tian, X.; Zhao, X.; Wang, M.; Wang, Z. Effective suppression of stimulated Raman scattering in direct laser diode pumped 5 kilowatt fiber amplifier using chirped and tilted fiber bragg gratings. *Laser Phys. Lett.* **2020**, *17*, 085104. [CrossRef]
18. Lin, W.; Desjardins-Carrière, M.; Sévigny, B.; Magné, J.; Rochette, M. Raman suppression within the gain fiber of high-power fiber lasers. *Appl. Opt.* **2020**, *59*, 9660–9666. [CrossRef]
19. Wang, Z.; Wang, M.; Hu, Q. Filtering of stimulated Raman scattering in a monolithic fiber laser oscillator using chirped and tilted fiber Bragg gratings. *Laser Phys.* **2019**, *29*, 075101. [CrossRef]
20. Wang, M.; Li, Z.; Liu, L.; Wang, Z.; Xu, X. Suppression of stimulated Raman scattering in two-stage high-power 1090 nm fibre amplifier using chirped and tilted fibre Bragg gratings. *Laser Phys.* **2018**, *28*, 125102. [CrossRef]
21. Wang, M.; Liu, L.; Wang, Z.; Xi, X.; Xu, X. Mitigation of stimulated Raman scattering in kilowatt-level diode-pumped fiber amplifiers with chirped and tilted fiber Bragg gratings. *High Power Laser Sci. Eng.* **2019**, *7*, e18. [CrossRef]
22. Jiao, K.; Shu, J.; Shen, H.; Guan, Z.; Yang, F.; Zhu, R. Fabrication of kW-level chirped and tilted fiber Bragg gratings and filtering of stimulated Raman scattering in high-power CW oscillators. *High Power Laser Sci. Eng.* **2019**, *7*, e31. [CrossRef]
23. Lemaire, P.; Atkins, R.; Mizrahi, V.; Reed, W. High-Pressure H-2 Loading as a Technique for Achieving Ultrahigh UV Photosensitivity and Thermal Sensitivity in Geo2 Doped Optical Fibers. *Electron. Lett.* **1993**, *29*, 1191–1193. [CrossRef]
24. Yan, Z.; Wang, H.; Wang, C.; Sun, Z.; Yin, G.; Zhou, K.; Wang, Y.; Zhao, W.; Zhang, L. Theoretical and experimental analysis of excessively tilted fiber gratings. *Opt. Express* **2016**, *24*, 12107–12115. [CrossRef] [PubMed]
25. Albert, J.; Shao, L.-Y.; Beliaev, A.; Caucheteur, C. Polarization Properties of Tilted Fiber Bragg Gratings for Novel Sensing Modalities. In *Fiber Optic Sensors and Applications VIII*; Mihailov, S.J., Du, H.H., Pickrell, G., Eds.; International Society for Optics and Photonics: Orlando, FL, USA, 2011; p. 802802.